Proceedings of the 28th IEEE
EMBS Annual International Conference
New York City, USA, Aug 30-Sept 3, 2006

Endocardium and Epicardium Contour Modeling Based on Markov Random Fields and Active Contours

Lucilio Cordero-Grande, Pablo Casaseca-de-la-Higuera, Marcos Martín-Fernández and Carlos Alberola-López

Abstract— **A segmentation application prototype of the volume of the left ventricle for Magnetic Resonance Imaging is being developed. The foundation for this work is given by modeling possible radial deformations of the epicardium and endocardium contours by means of a Markov Random Field over which the most probable configuration is estimated. The field makes use of a Bayesian approach based on *a priori* terms which impose smoothness along the coupled contours and likelihood terms which gather information provided by the images about the areas where the contours are supposed to be. The parameters of the field are estimated on a supervised basis.**

I. INTRODUCTION

Myocardial function characterization is a problem of paramount importance from all perspectives. Heart failures show big rates of mortality in modern life [1] so correct perfusion after a heart stroke and even myocardial regeneration (via, for instance, stem cells) are the focus of the effort in many medical centers all over the world. In this scenario, automated means to characterize myocardial function are desirable, since they provide objective (repeatable) results, which aim at analyzing, with scientific rigor, the pros and cons of different medical treatments.

In this paper we will face this problem by pursuing an automatic segmentation of the epicardium and endocardium from a volumetric set of short-axis Magnetic Resonance (MR) images. The problem here addressed is, by no means, a new one, but the solution proposed, to our knowledge, will show novel ingredients. Actually, the problem we deal with has been faced by many others. Several approaches propose to use a model-based segmentation [2], as we do. In [3] a volumetric atlas matching was performed and the authors use 4D information. In [4] the authors use a shape constrained deformable model which directly finds a segmentation in 3D. Difficulties may arise, however, when a significant shift between adjacent slices is present, due to breathing. In [5], an active contour framework, which shares the general philosophy of our work, is optimized by means of an annealing scheme; however the parameters involved do not seem to be estimated from available data.

The authors acknowledge the Comisión Interministerial de Ciencia y Tecnología for research grant TEC2004-06647-C03-01, the Fondo de Investigaciones Sanitarias for grant PIO-41483, the Junta de Castilla y León for grant VA075A05 and the European Commission for the funds associated to the Network of Excellence SIMILAR (FP6-507609). The authors acknowledge the ICICOR (Instituto de Ciencias del Corazón, Valladolid, Spain) and the Centro PET Recoletas Valladolid for the expertise exchange as well as the data provided to carry out this research. The authors are with the Laboratorio de Procesado de Imagen (LPI), Escuela Técnica Superior de Ingenieros de Telecomunicación, University of Valladolid, 47011 Valladolid, España. {lcorgra,casaseca}@lpi.tel.uva.es, {marcma,caralb}@tel.uva.es

In this paper we propose a model-based segmentation procedure which is based on active contours and Markov Random Fields (MRF). Our solution is an adaptation of one previously developed for automatic extraction of kidney contours [6] in ultrasound images, which, in turn, was somehow inspired by the framework proposed in [7] for the 2D+T segmentation of endocardial and epicardial boundaries. In this paper, however we will analyze how a generic model to detect hard-to-tell boundaries (which is the case in ultrasound images) for star-like objects can be adapted to a different problem. Specifically, we focus on the problem of supervised parameter estimation from labeled data to determine whether the modeling terms are really needed or some of them may be removed or modified. Additionally, a new term (with respect to the model in [6]) is proposed to account for the joint presence of the two contours.

Section II introduces the definitions needed in the paper and then both the prior and the likelihood functions of the model are described. Section III presents some quantitative results of the estimation of the model parameters and visual results of the segmentation of the contours. Section IV summarizes the paper together with some concluding remarks.

II. DESCRIPTION

Our objective is to create a probabilistic model of the deformations of initial contours to eventually determine the contours of endocardium and epicardium out of a series of cardiac MR slices. To that end, a 2D MRF is defined, which favors contour smoothness and that aims at keeping the myocardium thickness constant within the same slice.

A. Initial model fitting

As for initialization, we use the 3D Slicer functionalities [8] to load the images and insert a point corresponding to the vertex of the left ventricle (LV). Then, an initial model, constituted by two concentric circumferences, is automatically positioned in the image, and then refined to obtain the estimated contours as indicated below. The center of the result is now propagated to the next slice and the process is repeated until the heart base is reached.

For circumferences positioning first a radial edge detector detects two candidate points for the endocardium boundary in several directions. Detection of two points is necessary to avoid a negative influence of the papillary muscles in the fitting. For both points, a correspondent epicardium boundary is also detected if the image contains enough information in that direction. Then the two clouds of points so generated are

assumed to belong to two concentric circumferences which are fitted by means of a least-square procedure [9].

B. Active rays. A discrete solution

For every image, each contour is parameterized by $J(p)$ rays that start off its center $\mathbf{C}(p)$ and cover completely and homogeneously the 2π-radian span. Index p ranges within the interval $[1,P]$ with P the number of slices inspected. Angular and radial initial components are represented by $\boldsymbol{\theta}(p)=\theta_j$ and $\boldsymbol{\rho}(p)=\rho^i$, where $1\leq j\leq J(p)$ and $i=\{1,2\}$, with $i=1$ related to the endocardium contour and $i=2$ to that of the epicardium. The resulting contour is obtained by finding the appropriate deformation in the radial coordinate with respect to the initial contour; such deformation, for each contour (i), ray position (j) and slice (p) is referred to as $\boldsymbol{d\rho}(p)=d\rho^i_j$. So we have two surfaces, each one approximated by P planar contours constituted by $J(p)$ elements. These deformations are able to take on, for each slice, ray and contour, one among $K(p)$ uniformly defined values

$$dr_k = 3\frac{k-1}{2(K-1)}w - w \tag{1}$$

in the radial surroundings $[\rho^i - w, \rho^i + \frac{w}{2}]$, with $1\leq k\leq K(p)$, where $w=\rho^2-\rho^1$, the radial distance between the initial contours. We illustrate these parameters graphically in Fig. 1.

C. The prior

In order to build a prior model we have followed the criterion to give a greater probability to those deformations that generate as solutions contours with forms of membrane type (first derivative smoothness) and thin flat lamina type (second derivative smoothness). Such derivatives are approximated by means of finite differences.

For now we drop the index p of our expressions, which corresponds to select one of the slices. The deformations field is constituted by a bidimensional MRF for each slice of such form that $|\mathbf{S}|=2J$, where $\mathbf{S}$ is the set of locations of the field. $dw^i_j = dw_{\mathbf{s}}$ is the random variable that represents the deformation for each position, which takes on values in a space of possible configurations $\boldsymbol{\Lambda}=\{dr_k\}$. $\boldsymbol{d\rho}$ is a sample of the field and therefore $\boldsymbol{d\rho}\in\boldsymbol{\Omega}$ where the latter is the space of possible deformations. We define a neighborhood system $\boldsymbol{\partial}$ non-isotropic and cyclical in both components, which, for a certain position $\mathbf{s}=(j,i)$, can be expressed as

$$\begin{aligned}\boldsymbol{\partial}(\mathbf{s}) = \{&(j-2,i),(j-2,i-1),(j-1,i),(j-1,i-1),\\ &(j,i-1),(j+1,i),(j+1,i-1),(j+2,i),(j+2,i-1)\}.\end{aligned} \tag{2}$$

In our model we are interested in four clique categories that belong to the set $\boldsymbol{\mathscr{C}}$ of the cliques induced by the neighboring system. They are presented in Fig. 2. With their respective elements we approximate four derivatives, namely, the first and second order derivatives (in the angular direction) of the deformation $d\rho^i_j$ as well as the first and second order derivatives (in the angular direction) of the difference of the deformation in the two contours $d\rho^i_j - d\rho^{i-1}_j$. The model, as indicated above, favors smoothness not only in every contour but also in the thickness of the myocardial wall.

Each of the derivative enters the prior by means of an associated potential function

$$\Psi_l(\phi_l) = \nu_l|\phi_l|^{\beta_l}, \tag{3}$$

with $\nu_l\geq 0$, $0\leq\beta_l\leq 1$, and $l=\{1,2,3,4\}$ that induces a measurement of a priori probability Π^{pri} in the space $\boldsymbol{\Omega}$ for the Gibbs Field (GF) $\mathbf{dw}$ with respect to the neighborhood system $\boldsymbol{\partial}$. The energy function of the field is determined as

$$H(\boldsymbol{d\rho}) = \sum_{\mathbf{C}\in\boldsymbol{\mathscr{C}}} \Psi_{\mathbf{C}}(\boldsymbol{d\rho}_{\mathbf{C}}), \tag{4}$$

the conditional probability function can be expressed as

$$\Pi^{pri}(dw_{\mathbf{s}} = dr_k | dw_{\mathbf{t}} = d\rho_{\mathbf{t}}, \mathbf{t}\in\boldsymbol{\partial}(\mathbf{s})) = \frac{\exp(H(d\rho_{\mathbf{s}}))}{\sum_{z_{\mathbf{s}}\in\boldsymbol{\Lambda}}\exp(H(z_{\mathbf{s}}))}. \tag{5}$$

D. Likelihood function

The likelihood function is basically that used in [6]. For the sake of completeness we include here a brief description as well as the necessary definitions.

1.- Definitions. Every image $\mathbf{I}$ has a size $M\times N$. In the natural image coordinate system the center of the contours is denoted as $\mathbf{C}_p=(C_m,C_n)$. $\mathbf{Z}(m,n)$ is a complex representation for the contour so that the origin corresponds to the center of the contour.

The presence of the contours is visually recognized from the MR images by two mechanisms. On one hand, the myocardium is allocated in an intensity homogeneous zone between an inner clearer one and an outer generally clearer one. On the other hand the contours are locally appraised by those two changes in intensity. This is what is used to determine the two main subsets of the image that contain the image information we will employ (see Fig. 1):

a) *Angular sector with proximity to the contour.* The set is denoted as $\beta^i(k,j)$. It is constituted by the pixels whose phase $\angle\mathbf{Z}(m,n)$, is the nearest to θ_j and they are radially positioned the nearest with respect to the deformed point ρ^i+dr_k. The union of these sets in k is what we denominate *Region Of Deformation* of a point $ROD^i(j)$, so $\beta^i(j,k)$ is a partition of $ROD^i(j)$.

b) *Angular sector external/internal to the contour.* The set is denoted as $\gamma^i(k,j)$ and its pixels are those ones that, being included in $ROD^i(j)$ satisfy that $|\mathbf{Z}(m,n)|\geq\rho^1+dr_k$ or $|\mathbf{Z}(m,n)|\leq\rho^2+dr_k$ respectively for endocardial and epicardial contours.

2.- Intensity Image. The model function must approximate the expectable characteristics of the images. A Beta probability density function can accomplish that objective, because its parameters α_1 and α_2 allow a wide model range of probabilistic distributions. We define a Beta function of the image pixels conditioned to the deformation $f^i_B(I(m,n)|dw^i_j=dr_k)$, with dw^i_j the random variable of the deformation with respect to each ray, slice and contour and $(m,n)\in\gamma^i(k,j)$. The parameters must be estimated for each ray, slice and contour.

We do a preprocessing similar to that on [6] and apply the method of the moments, as the parameters are not critical and are functionally related to the mean and the variance of the distribution.

3.- Edge Image. This image is related to the gradient of the original one by means of a preprocessing, that will basically consist of smoothing that gradient and masking the result (so the masked image contains only those regions in which the intensity trend in the radial direction takes the sign that the contour is supposed to take with the considerations we made about visually recognition of contours). We denote this smoothed gradient by $B(m,n)$. It is used an exponential model $f_E^i(B(m,n)|dw_j^i = dr_k)$.

4.- Joint Model. From the previous images of intensity I and edge B, we can construct the joint probability density functions $f^i(\mathbf{I},\mathbf{B}|\mathbf{dw}^i = \boldsymbol{d\rho}^i)$, which we suppose conditionally independent, where $\mathbf{dw}^i$ is the variable that represents the set of possible deformations on every slice. This functions define the likelihood of the images conditioned to the position of each of the surfaces, but operativeness is achieved only if we simplify them. If besides the already implicitly supposed conditional independence between slices and between contours, we suppose there exists conditional independence between sectors, between intensity and gradient, among adjacent pixels and independence of values external to γ and β, we obtain the next identity (details can be consulted on [6])

$$\begin{aligned} f^i(\mathbf{I},\mathbf{B}|\mathbf{dw}^i = \boldsymbol{d\rho}^i) = \\ \prod_j \prod_{(m_1,n_1)\in\gamma^i(k,j)} f_B^i(I(m_1,n_1)|dw_j^i = dr_k) \\ \prod_{(m_2,n_2)\in\beta^i(k,j)} f_E^i(B(m_2,n_2)|dw_j^i = dr_k). \end{aligned} \tag{6}$$

We can introduce the previously defined probability density functions of the intensity and edge images to complete our model of likelihood. As it will be stated later, we are interested in the logarithmic probability functions

$$\begin{aligned} L_{\mathbf{I}}^i(k,j) = \frac{1-\alpha_2(j)}{|\gamma^i(k,j)|} \cdot \sum_{(m,n)\in\gamma^i(k,j)} \\ [\ln(1-I(m,n))) + \frac{1-\alpha_1(j)}{1-\alpha_2(j)} \ln(I(m,n))] \end{aligned} \tag{7}$$

$$L_{\mathbf{B}}^i(k,j) = -\frac{\sum_{(m,n)\in\beta^i(k,j)} B(m,n)}{|\beta^i(k,j)|}, \tag{8}$$

where $|A|$ represents the cardinality of A and it is used for normalization.

E. Complete model

The prior and likelihood functions are combined into the posterior by means of Bayes theorem. Since both are Gibbs functions, the net effect is to enlarge the prior function with an additional potential function with expression $\Psi_5(d\rho_{\mathbf{s}}) = v_5^i L_{\mathbf{I}}^i(k,j) + v_6^i L_{\mathbf{B}}^i(k,j)$. The new parameters weigh the importance of the data with respect to the prior model.

If the parameters v_l^i, $i = \{1,2\}$, $1 \le l \le 6$ were known, the configuration $\boldsymbol{d\rho}$ that maximizes Π^{pos} (the new induced probability function) is given by the maximum a posteriori estimator. This can be obtained by means of several algorithms. One of them, namely, the Simulated Annealing algorithm, is the one used in this paper. Details concerning this algorithm can be consulted in well-known references (see, for instance [10] and references therein). The major drawback of this algorithm is the time needed for convergence (so cooling schedules have been proposed to speed it up [11]) but since the configuration space is, in our case, relatively small, this has not been an issue.

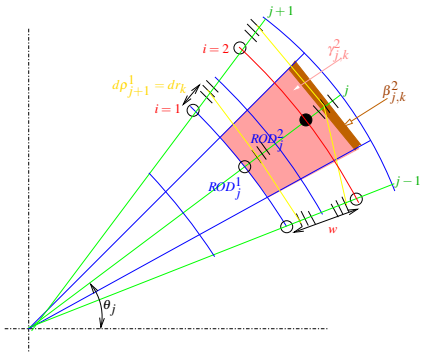

Fig. 1. Discretization of the surface and likelihood sets.

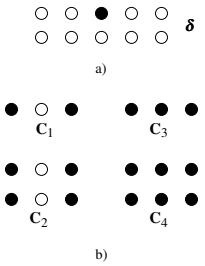

Fig. 2. a) Neighborhood system, b) clique categories used in the model.

F. Parameter estimation

The vector of the twelve parameters $\boldsymbol{v}$ remains unknown. In order to estimate them we resort to a supervised method in which a segmented volume data set is taken as ground truth.

As for the estimation itself one possible method is maximum likelihood i.e., the configuration over the parameter space for which

$$\boldsymbol{v}^* = \arg\max_{\boldsymbol{v}} \Pi^{pos}(\boldsymbol{dw} = \boldsymbol{d\rho}|\mathbf{I},\mathbf{B};\boldsymbol{v}). \tag{9}$$

It is well known [10], however, that this estimation involves a lot of computation due to the need of calculating the partition constant with the GF. An alternative is the maximum pseudo-likelihood estimator

$$\hat{\boldsymbol{v}} = \arg\max_{\boldsymbol{v}} \prod_i \prod_j \Pi^{pos}(dw_j^i = d\rho_j^i|\mathbf{I},\mathbf{B};\boldsymbol{v}). \tag{10}$$

This method along with a gradient descent algorithm (ascent in our case) is used to obtain the final estimate.

III. RESULTS

First, in order to analyze the variability of the optimization process with respect to the initial solution, we run the algorithm with an initial solution in which all the parameters take on random values within the range $[0,10]$ (say, solution $\boldsymbol{\nu}_0^r$) and another one (say $\boldsymbol{\nu}_0^u$) in which all of them take on the value 5. Results are shown in Table I, where e denotes the mean relative difference between the estimations; clearly, for low values of p (near the apex) in which the contours are fairly small results are more unstable. As the algorithm progresses and analyzes more centered slices of the heart results show greater stability.

Second, the parameters are analyzed. We noted that for some slices, there is a null influence of some potential terms as parameters converge to zero. Overall influences are presented by taking the percentage of images in which each term influences the field as in Table II. We can conclude that every term of the model seems to contribute to the proposed field, but that the edge likelihood term for the epicardium needs to be refined, what arises from the fact that the myocardium external structures are heterogeneous.

To illustrate the interest of the model, we present the results of the segmentation by estimation of parameters in a collection of sets of training volume images and segmentation on another set. From a total of three sets, two are used for training and the other one for evaluation. The estimated parameters are averaged along slices and the result is used for segmentation. In Fig. 3 a representative slice of each set is included. From the left to the right, the images go from the base to the apex. The automatic segmentation is in red and the manual one in green. In the left and central images a representative number of matches occurs, and deviations are small, but in the right image the results are worse; as it has been stated, the model is more appropriate for slices of the LV in which more data are available for estimations.

TABLE I

MEAN RELATIVE DIFFERENCE OF CONVERGENCE VALUES FOR EACH IMAGE

p	1	2	3	4	5	6
	7	8	9	10	11	-
e	1.42e-2	3.45e-1	1.68e-2	4e-4	9e-4	3e-4
	5e-4	1.6e-3	1.65e-2	1.3e-3	4.2e-3	-

TABLE II

PERCENTAGE OF IMAGES IN WHICH THE TERM INFLUENCES THE FIELD

ϕ_1^1	ϕ_2^1	ϕ_3^1	ϕ_4^1	L_I^1	L_B^1
54.1%	100%	70.8%	70.8%	70.8%	91.6%
ϕ_1^2	ϕ_2^2	ϕ_3^2	ϕ_4^2	L_I^2	L_B^2
79.1%	95.8%	79.1%	83.3%	91.6%	50.0%

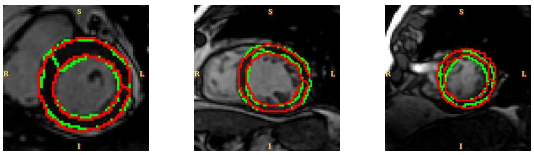

Fig. 3. Segmentation results

IV. CONCLUSIONS AND FUTURE WORKS

In this paper we have proposed a method to find the contours of both the endocardium and the epicardium out of a number of MR images. Our purpose was to adapt an existing method previously published to the problem here described. To that end additional terms which force smoothness in myocardium thickness along each image were introduced. Modeling parameters were estimated from data to account for the appropriateness of each term in the overall model. Some examples graphically illustrated that the parameter estimates seemed correct in terms of segmenting capability of the model. The next step would be to accomplish a fully automated process in which segmentation and parameter estimation would be carried out simultaneously.

The likelihood model proposed in this paper should be improved; although its influence in the parameter estimation is comparable to that of the prior model, statistics of MR images are well-known and more mathematically tractable than those needed in ultrasound, so the choice of a Beta distribution is, for this problem, not so well justified. Further efforts would pursue these ideas.

REFERENCES

[1] American Heart Association, Heart and stroke statistical update, *http://www.americanheart.org*, 2001.

[2] A. F. Frangi, W. J. Niessen and M. A. Viergever, Three-Dimensional Modeling for Functional Analysis of Cardiac Images: A Review, *IEEE Transactions on Medical Imaging*, vol. 20, 2001, pp. 2–25.

[3] M. Lorenzo-Valdes, G. I. Sanchez-Ortiz, A. G. Elkington, R. H. Mohiaddin D. Rueckert, Segmentation of 4D Cardiac MR Images using a Probabilistic Atlas and the EM Algorithm, *Medical Image Analysis*, vol. 8, 2004, pp. 255–265.

[4] M. R. Kaus, J. von Berg, J. Weese, W. Niessen V. Pekaret, Automated Segmentation of the Left Ventricle in Cardiac MRI, *Medical Image Analysis*, vol. 8, 2004, pp. 245–254.

[5] C. Pluempitiwiriyawej, J. M. F. Moura, L. W. Yi-Jen, H. Chien, STACS: New Active Contour Scheme for Cardiac MR Image Segmentation, *IEEE Transactions on Medical Imaging*, vol. 24, 2005, pp. 593–603.

[6] M. Martin-Fernandez and C. Alberola-Lopez, An Approach for Contour Detection of Human Kidneys from Ultrasound Images using Markov Random Fields and Active Contours, *Medical Image Analysis*, vol. 9, 2005, pp. 1–23.

[7] J. M. Dias, J. M. N. Leitao, Wall Position and Thickness Estimation from Sequences of Echocardiographic Images, *IEEE Transactions on Medical Imaging*, vol. 15, 1996, pp. 25–38.

[8] 3D Slicer, *www.slicer.com*, 2005.

[9] P. O'Leary, M. Harker, P. Zsombor-Murray, Direct and Least Square Fitting of Coupled Geometric Objects for Metric Vision, *IEE Proceedings on Vision, Image and Signal Processing*, vol. 152, 2005, pp. 687–694.

[10] S. Z. Li, *Markov Random Field Modeling in Computer Vision*, Springer Verlag, Berlin, Germany, 1995.

[11] B. Hajek, Cooling Schedules for Optimal Annealing, *Mathematics of Operations Research*, vol. 13, 1988, pp. 311–329.